

# VE-cadherin interacts with cell polarity protein Pals1 to regulate vascular lumen formation

Benjamin F. Brinkmann<sup>a,b,c</sup>, Tim Steinbacher<sup>a,b</sup>, Christian Hartmann<sup>a,b,c</sup>, Daniel Kummer<sup>a,b,c</sup>, Denise Pajonczyk<sup>a,b</sup>, Fatemeh Mirzapourshafiyi<sup>d</sup>, Masanori Nakayama<sup>d</sup>, Thomas Weide<sup>e</sup>, Volker Gerke<sup>b,f</sup>, and Klaus Ebnet<sup>a,b,c,\*</sup>

<sup>a</sup>Institute-Associated Research Group "Cell Adhesion and Cell Polarity," <sup>b</sup>Institute of Medical Biochemistry, Center for Molecular Biology of Inflammation, and <sup>c</sup>Interdisciplinary Clinical Research Center, University of Münster, 48419 Münster, Germany; <sup>d</sup>Laboratory for Cell Polarity and Organogenesis, Max Planck Institute for Heart and Lung Research, 61231 Bad Nauheim, Germany; <sup>e</sup>Department of Internal Medicine D, Division of Molecular Nephrology, University Hospital Münster, Albert-Schweitzer-Campus 1, and <sup>f</sup>Cells-in-Motion Cluster of Excellence (EXC 1003-CiM), University of Münster, 48419 Münster, Germany

**ABSTRACT** Blood vessel tubulogenesis requires the formation of stable cell-to-cell contacts and the establishment of apicobasal polarity of vascular endothelial cells. Cell polarity is regulated by highly conserved cell polarity protein complexes such as the Par3-aPKC-Par6 complex and the CRB3-Pals1-PATJ complex, which are expressed by many different cell types and regulate various aspects of cell polarity. Here we describe a functional interaction of VE-cadherin with the cell polarity protein Pals1. Pals1 directly interacts with VE-cadherin through a membrane-proximal motif in the cytoplasmic domain of VE-cadherin. VE-cadherin clusters Pals1 at cell-cell junctions. Mutating the Pals1-binding motif in VE-cadherin abrogates the ability of VE-cadherin to regulate apicobasal polarity and vascular lumen formation. In a similar way, deletion of the Par3-binding motif at the C-terminus of VE-cadherin impairs apicobasal polarity and vascular lumen formation. Our findings indicate that the biological activity of VE-cadherin in regulating endothelial polarity and vascular lumen formation is mediated through its interaction with the two cell polarity proteins Pals1 and Par3.

**Monitoring Editor**  
Thomas M. Magin  
University of Leipzig

Received: Feb 26, 2016  
Revised: Jul 15, 2016  
Accepted: Jul 19, 2016

## INTRODUCTION

Many organs are composed of sheets of cells wrapped into tubes that can form either simple pipes such as the intestine or the kidney

This article was published online ahead of print in MBoc in Press (<http://www.molbiolcell.org/cgi/doi/10.1091/mboc.E16-02-0127>) on July 27, 2016.

The authors declare that they have no conflict of interest.

B.F.B. and K.E. designed and conceived the study. B.F.B. performed most of the experimental work. T.S., C.H., D.K., D.P., and F.M. performed experiments. T.W. provided important reagents. B.F.B., M.N., V.G., and K.E. analyzed the data. B.F.B. and K.E. wrote the manuscript.

\*Address correspondence to: Klaus Ebnet ([ebnetk@uni-muenster.de](mailto:ebnetk@uni-muenster.de)).

Abbreviations used: AJ, adherens junctions; aPKC, atypical protein kinase C; CBD, catenin-binding domain; Coll IV, collagen type IV; ECM, extracellular matrix; ERM, ezrin-radixin-moesin; HUVEC, human umbilical vein endothelial cells; JMD, juxtamembrane domain; p120ctn, p120 catenin; Pals1, protein associated with Lin-7; Par, partitioning defective; Podxl, podocalyxin; PtdIns, phosphatidylinositol; PTEN, Phosphatase and Tensin Homologue; TJ, tight junctions; VE-cadherin, vascular endothelial cadherin.

© 2016 Brinkmann et al. This article is distributed by The American Society for Cell Biology under license from the author(s). Two months after publication it is available to the public under an Attribution-NonCommercial-Share Alike 3.0 Unported Creative Commons License (<http://creativecommons.org/licenses/by-nc-sa/3.0>).

"ASCB®," "The American Society for Cell Biology®," and "Molecular Biology of the Cell®" are registered trademarks of The American Society for Cell Biology.

or an extensive network of tubes such as the tracheal system of invertebrates or the blood and lymphatic vasculature of vertebrates (Lubarsky and Krasnow, 2003). The inner surfaces of these tubes are lined with epithelial or endothelial cells. Both cell types are highly polarized, with well-developed apicobasal membrane polarity. The apical domain faces the lumen of the tube, the lateral membrane domain is in contact with neighboring cells, and the basal membrane domain adheres to the extracellular matrix (ECM; Yeaman et al., 1999). The formation of biological tubes is intimately linked to the development of apicobasal membrane polarity (Zegers et al., 2003; Martin-Belmonte et al., 2008; Lampugnani et al., 2010), and loss of cell polarity is frequently associated with defects in organ formation or cancer development (McCaffrey and Macara, 2011; Rodriguez-Boulan and Macara, 2014).

In epithelial cells, apicobasal polarity is regulated by a conserved set of polarity protein complexes. These include the Par3-atypical protein kinase C (aPKC)-Par6 complex (Par complex), the CRB3-Pals1-PATJ complex (CRB3 complex), and the Scribble-Lgl-Dlg complex (Scrb complex; Macara, 2004). The Par complex and the CRB3 complex localize to the apical region of the intercellular junctions, which harbors the tight junctions (TJs)

in vertebrates, whereas the Scrb complex localizes to the basolateral membrane domain (Macara, 2004). The Par complex and the CRB3 complex are biochemically linked through a direct association between Par6 and Pals1 (Hurd *et al.*, 2003; Wang *et al.*, 2004).

The endothelium represents a simple squamous epithelium that lines the surface of blood and lymphatic vessels. Endothelial cells are polarized and are connected by intercellular junctions that contain TJs and adherens junctions (AJs; Dejana, 2004). As opposed to epithelial cell–cell junctions, where the TJs are concentrated at the apical region of the junction and separated from the AJs, the TJs of endothelial cells are localized along the entire lateral junctional cleft and are intermingled with AJs and gap junctions (Simionescu *et al.*, 1975, 1976). Accordingly, proteins that in epithelial cells are separated by their specific localization in TJs and AJs, including occludin, ZO-1, or claudins, and cadherins or catenins, respectively, colocalize at endothelial cell–cell contacts (Schulze and Firth, 1993; Vorbrodt and Dobrogowska, 2003; Ruffer *et al.*, 2004).

Despite a similar molecular composition of cell–cell junctions in epithelial cells and endothelial cells, the mechanisms regulating cellular polarity and lumen formation are much less understood in endothelial cells. The major cell adhesion molecule at endothelial cell–cell junctions—vascular endothelial (VE)-cadherin—directly interacts with components of the Par complex (Iden *et al.*, 2006; Lampugnani *et al.*, 2010; Tyler *et al.*, 2010) and regulates the localization of the Par complex regulator Tiam1, as well as the activity of aPKC at cell–cell junctions (Lampugnani *et al.*, 2002, 2010), suggesting a specific role in endothelial polarization. In the absence of VE-cadherin, endothelial cells fail to develop a polarized vascular lumen both *in vitro* and *in vivo* (Lampugnani *et al.*, 2010). The activity of VE-cadherin in regulating endothelial polarization and vascular lumen formation has been partially linked to its association with cerebral cavernous malformations (CCMs) 1/Krev interaction trapped (Krit) 1 protein (Lampugnani *et al.*, 2010). The physiological implications of its association with cell polarity proteins are not well understood.

Here we describe an interaction of VE-cadherin with the polarity protein Pals1. Pals1 is a member of the membrane-associated guanylate kinase family of scaffold proteins, which are characterized by a specific arrangement of protein–protein interaction domains, including PSD-95/Dlg/ZO-1 (PDZ) domains, Src homology-3 (SH3) domains, Lin-2/Lin-7 (L27) domains, WW domains, and guanylate kinase domains (Funke *et al.*, 2005). In epithelial cells, Pals1 is localized at TJs, where it links the integral membrane protein CRB3 to the multiple PDZ domain–containing scaffold protein Protein Associated with Tight Junctions (PATJ) to form the tripartite CRB3-Pals1-PATJ complex (Roh *et al.*, 2002; Makarova *et al.*, 2003). Pals1 also directly interacts with Par6 through a conserved motif that is not involved in the interactions with CRB3 and PATJ, and this association regulates the localization of these two polarity complexes at the TJs in a mutual way (Hurd *et al.*, 2003; Wang *et al.*, 2004). Loss of Pals1 expression in Madin–Darby canine kidney (MDCK) cells results in delayed polarization, impaired barrier function, and defective lumen formation (Roh *et al.*, 2003; Straight *et al.*, 2004). We find that VE-cadherin directly interacts with Pals1 and promotes the recruitment of Pals1 to intercellular junctions. Of importance, VE-cadherin mutants that cannot directly interact with Pals1, as well as VE-cadherin mutants that cannot directly interact with Par3, fail to support normal lumen development in three-dimensional (3D) culture. Our findings provide a molecular basis for the role of VE-cadherin during vascular lumen formation.

## RESULTS

### The cell polarity protein Pals1 interacts with VE-cadherin in vascular endothelial cells

Given previous reports describing VE-cadherin as protein interacting with various polarity proteins, including Par3 and Par6 (Iden *et al.*, 2006; Lampugnani *et al.*, 2010; Tyler *et al.*, 2010; Liu *et al.*, 2013), we tested whether VE-cadherin associates with the cell polarity protein Pals1. We first analyzed the expression of Pals1 in endothelial cells by Western blotting and immunoprecipitation (IP). We found that human umbilical vein endothelial cells (HUVECs) express two Pals1 isoforms corresponding to relative molecular masses ( $M_r$ ) of ~82 and 72 kDa (Figure 1A), which is similar to what is found in epithelial cells (Straight *et al.*, 2004; Cao *et al.*, 2005). We next addressed the interaction between VE-cadherin and Pals1 by coIP experiments. VE-cadherin immunoprecipitates obtained from HUVECs contained the 82-kDa Pals1 isoform which is considered the canonical Pals1 isoform ([www.uniprot.org/uniprot/Q8N3R9](http://www.uniprot.org/uniprot/Q8N3R9); Figure 1B). In addition, Pals1 immunoprecipitates obtained from transfected HEK293T cells contained VE-cadherin (Figure 1C). To further corroborate these findings, we analyzed the expression and localization of Pals1 in cultured cells and endothelial tissues. Pals1 colocalized with VE-cadherin at intercellular junctions of cultured HUVECs (Figure 1D) and with VE-cadherin at cell–cell junctions after ectopic expression in HEK293T cells (Figure 1E). In addition, Pals1 was coexpressed with VE-cadherin in endothelial cells of the vascular plexus in the mouse retina at postnatal day 6, as revealed by whole-mount staining of the retinal vasculature (Figure 1F). Together these findings indicate that Pals1 exists in a complex with VE-cadherin that localizes at endothelial cell–cell contacts.

To analyze whether the interaction between VE-cadherin and Pals1 is direct, we performed glutathione *S*-transferase (GST)–pull-down experiments using recombinant GST-fusion proteins encoding the cytoplasmic tail of VE-cadherin, which we incubated with [<sup>35</sup>S] methionine-labeled Pals1 generated *in vitro* using a coupled transcription/translation reticulocyte lysate system. The GST–VE-cadherin fusion protein precipitated Pals1 from reticulocyte lysates, indicating that the interaction with VE-cadherin is direct (Figure 1G). GST-fusion proteins containing the cytoplasmic domains of E-cadherin or N-cadherin did not precipitate Pals1 in the same system, indicating that Pals1 interacts specifically with VE-cadherin (Figure 1G). The cytoplasmic domain of VE-cadherin consists of three major regions: a juxtamembrane domain (JMD), which contains the binding site for p120ctn; a middle region; and a C-terminal catenin-binding domain (CBD), which interacts with  $\beta$ - and  $\gamma$ -catenin (Vincent *et al.*, 2004). The JMD and the CBD are conserved among classical cadherins, whereas the intervening region is less well conserved (Suzuki *et al.*, 1991; Tanihara *et al.*, 1994). We previously found that Par3 interacts with the C-terminal PDZ domain–binding motif of VE-cadherin (-EELIICOOH), whereas Par6 interacts with the JMD region through a site that is distinct from the p120ctn-binding site (Iden *et al.*, 2006). To identify the binding site of Pals1 in VE-cadherin, we performed GST-pull-down experiments with GST–VE-cadherin fusion proteins encompassing the JMD and part of the intervening region, the intervening region, or the CBD of the cytoplasmic domain of VE-cadherin. Pals1 interacted with the VE-cadherin construct representing the JMD and part of the intervening region but not with constructs representing the intervening sequence alone or the CBD (Figure 1I, top). To further characterize the binding site in VE-cadherin, we introduced triple-alanine mutations in the region flanking the p120ctn-binding site within the JMD of VE-cadherin. Mutating amino acids located C-terminal to the p120ctn-binding region partially reduced but did not abolish Pals1 binding (Figure 1I, bottom). On the other hand,

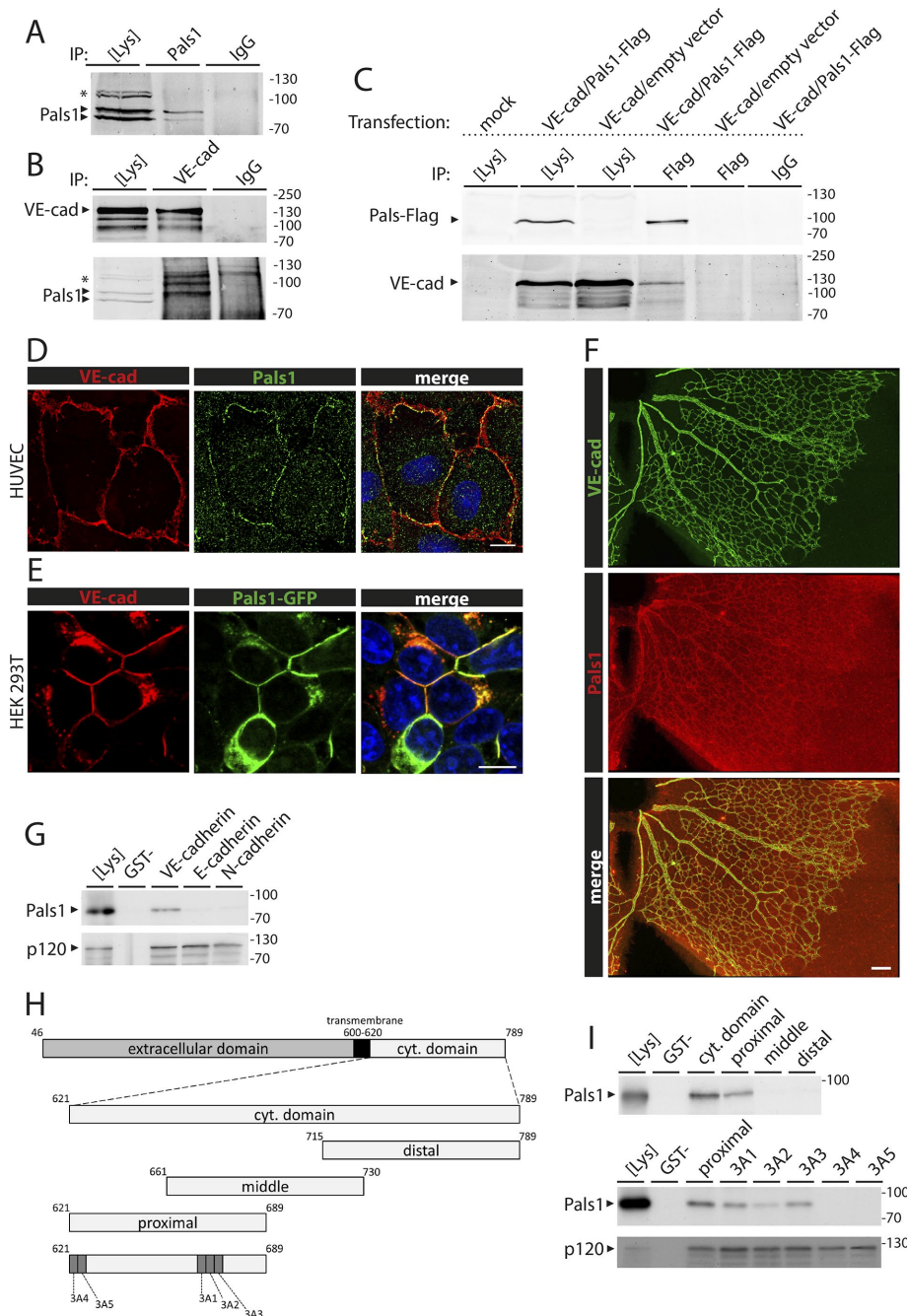


**FIGURE 1:** VE-cadherin exists in a complex with Pals1. (A) Pals1 expression in cultured endothelial cells. HUVEC lysates were analyzed for Pals1 expression by either direct Western blot analysis (lane 1) or IP followed by Western blot analysis (lane 2). IPs with isotype-matched control antibodies (lane 3) served as control. Pals1 appears as a doublet of bands reflecting the 82- and 72-kDa isoforms described in epithelial cells. Asterisks indicate unspecific bands. (B) CoIP of Pals1 and VE-cadherin. Top, 10% of immunoprecipitates obtained with antibodies against VE-cadherin (VE-cad, lane 2) or with isotype-matched control antibodies (IgG, lane 3) were incubated with anti-VE-cadherin antibodies to demonstrate efficiency of VE-cadherin IP. Bottom, immunoprecipitates obtained with antibodies against VE-cadherin were incubated with anti-Pals1 antibodies. VE-cadherin immunoprecipitates contain the 82-kDa isoform of Pals1. Lysates of HUVECs (Lys, lane 1) were loaded for comparison. Asterisks indicate unspecific bands. (C) CoIP of Pals1 and VE-cadherin after ectopic expression in HEK293T cells. HEK293T cells transfected with plasmids encoding Flag-tagged Pals1 (Pals1-Flag) and VE-cadherin (VE-cad) were incubated with antibodies against Pals1. Immunoprecipitates obtained with anti-Flag antibodies were immunoblotted with antibodies against Pals1 to demonstrate efficiency of Flag-Pals1 IP (10% of immunoprecipitate, top), or with antibodies against VE-cadherin (90% of immunoprecipitate, bottom). Note that immunoprecipitates obtained from VE-cadherin–Pals1 double-transfected cells but not from VE-cadherin single-transfected cells

mutating the amino acids located N-terminal to the p120ctn-binding region abolished the interaction. The interaction of VE-cadherin with p120ctn was not affected by these mutations (Figure 1I, bottom), suggesting that Pals1 and p120ctn do not compete for VE-cadherin binding. These observations indicate that Pals1 binding to VE-cadherin requires a short motif (R<sub>621</sub>RRIRQ<sub>626</sub> in mouse VE-cadherin, R<sub>621</sub>RRLRK<sub>626</sub> in human VE-cadherin) located N-terminal to the p120ctn-binding site within the JMD of VE-cadherin.

### VE-cadherin recruits Pals1 to cell–cell contacts

To address whether VE-cadherin promotes the localization of Pals1 at cell–cell contacts, we analyzed the localization of Pals1 in HEK293T cells, which have a fibroblastic

contain VE-cadherin. (D) Colocalization of Pals1 with VE-cadherin at endothelial cell–cell junctions. HUVECs were stained for Pals1 and VE-cadherin as indicated. Pals1 partially colocalizes with HUVECs at cell–cell contacts (merge). Scale bar, 10  $\mu$ m. (E) Colocalization of Pals1 and VE-cadherin after ectopic expression. HEK293T cells were transiently transfected with plasmids encoding Pals1-GFP and VE-cadherin as indicated. Pals1 and VE-cadherin colocalize at cell–cell contacts. Scale bar, 10  $\mu$ m. (F) Pals1 is expressed in vascular endothelial cells in vivo. Whole-mount preparations of mouse retinas were stained with antibodies against VE-cadherin (green) and Pals1 (red). Pals1 is expressed by vascular endothelial cells in the vascular plexus. Scale bar, 110  $\mu$ m. (G) Direct interaction of Pals1 with VE-cadherin. GST-fusion proteins containing the cytoplasmic domains of VE-cadherin, E-cadherin, and N-cadherin were incubated with in vitro–translated, [<sup>35</sup>S]methionine-labeled Pals1. Pals1 interacts specifically with VE-cadherin. (H) Schematic representation of VE-cadherin deletion and mutant constructs used in this study. (I) Pals1 interacts with a membrane-proximal motif in the cytoplasmic domain of VE-cadherin. Top, GST-fusion proteins containing the entire cytoplasmic domain (cyt. domain) or the membrane-proximal, -middle, or -distal parts of the cytoplasmic domain were incubated with in vitro–translated Pals1. Pals1 interacts with the membrane-proximal domain of the VE-cadherin cytoplasmic tail. Bottom, GST-fusion proteins containing the membrane-proximal part of the cytoplasmic domain with triple alanine (3A) mutations were analyzed for association with in vitro–translated Pals1 and p120ctn. Mutating either aa R<sub>621</sub>–R<sub>622</sub>–R<sub>623</sub> to A<sub>621</sub>–A<sub>622</sub>–A<sub>623</sub> (3A4) or aa I<sub>624</sub>–R<sub>625</sub>–K<sub>626</sub> to A<sub>624</sub>–A<sub>625</sub>–A<sub>626</sub> (3A5; mouse VE-cadherin) abolished association with Pals1.

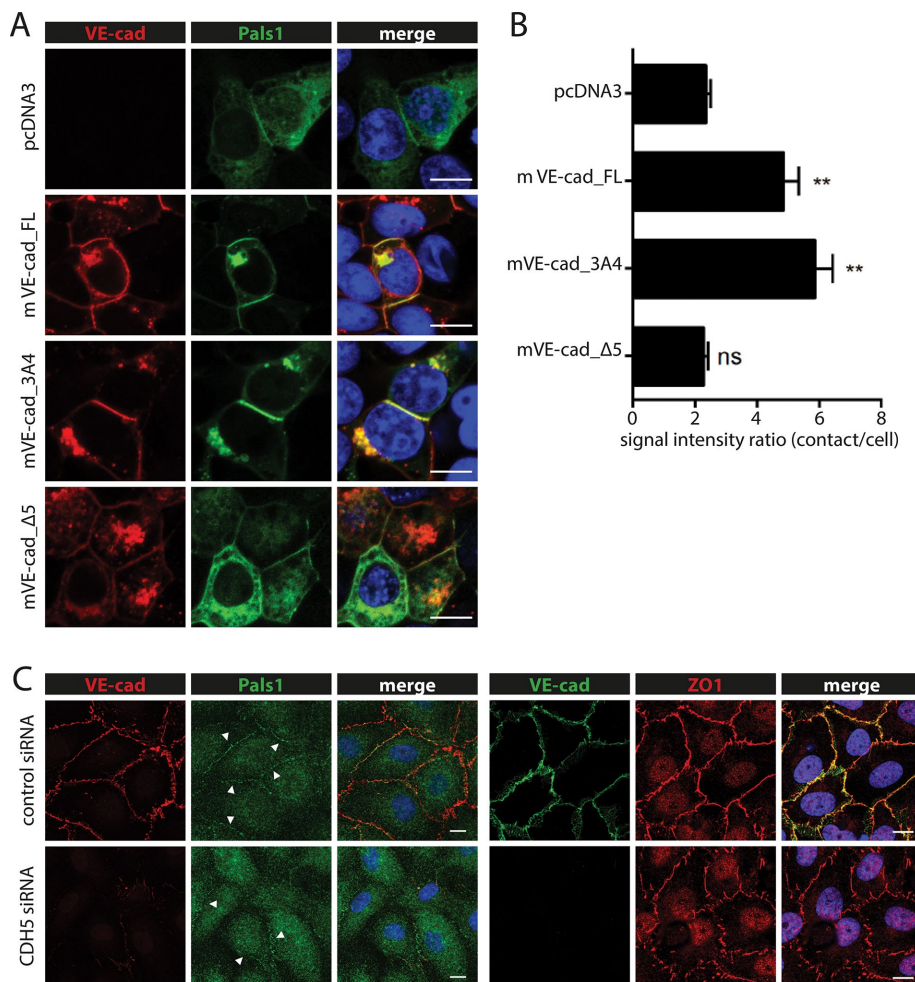


**FIGURE 2:** VE-cadherin recruits Pals1 to cell–cell contact sites. (A) Pals1 recruitment by VE-cadherin to cell–cell contacts. HEK293T cells were cotransfected with GFP-tagged Pals1 and various murine VE-cadherin constructs, including full-length VE-cadherin (mVE-cad\_FL), the Pals1 binding mutant of VE-cadherin (mVE-cad\_3A4), or the Par3 binding mutant of VE-cadherin (mVE-cad\_Δ5). VE-cadherin was visualized by indirect immunofluorescence; Pals1 was visualized using GFP fluorescence. Note that VE-cadherin recruits Pals1 to cell–cell contacts and that this activity depends on the PDZ domain–binding motif. Scale bars, 10 μm. (B) Statistical evaluation of Pals1 recruitment by VE-cadherin full-length and mutant constructs. The Pals1 signal intensity is given as ratio of signal intensity at cell–cell contacts and total signal intensities in the two contacting cells (see *Materials and Methods* for details). Quantitation of data shown here was performed using ANOVA with Dunnett’s test with 15 pictures analyzed for each condition and is presented as mean ± SEM; ns, not significant, \*\* $p < 0.0001$ . (C) Pals1 localization in VE-cadherin–knockdown cells. HUVECs transfected with control siRNA or VE-cadherin siRNA (CDH5 siRNA) were stained for VE-cadherin and Pals1 (left) or VE-cadherin and ZO-1 (right). Note that Pals1 localization is reduced but not completely abolished at cell–cell contacts of VE-cadherin–depleted cells. Arrowheads indicate Pals1 signals at cell–cell contact sites. Scale bars, 10 μm.

morphology (Dupre-Crochet *et al.*, 2007). When transfected alone, Pals1 was localized predominantly in the cytoplasm and only very weakly at cell–cell junctions, as indicated by a diffuse green fluorescent protein (GFP) signal throughout the cytoplasm and a weak GFP signal at cell boundaries (Figure 2A). When VE-cadherin was cotransfected with Pals1, the diffuse distribution of Pals1 in the cytoplasm was abolished and its junctional localization was strongly increased (Figure 2A), indicating that VE-cadherin promotes the localization of Pals1 at intercellular junctions. When we cotransfected Pals1 with the Pals1 binding mutant of VE-cadherin (VE-cad\_3A4), we observed enrichment of Pals1 at intercellular junctions, similar to that seen in cells cotransfected with wild-type (WT) VE-cadherin (Figure 2, A and B).

When Pals1 was cotransfected with the Par3 binding mutant of VE-cadherin (VE-cad\_Δ5), Pals1 was not enriched at cell–cell junctions but localized predominantly in the cytoplasm, similar to cells transfected with Pals1 alone (Figure 2, A and B). These observations indicate that VE-cadherin promotes Pals1 localization at intercellular junctions and that this activity is not mediated through the membrane-proximal motif involved in direct Pals1 binding but through the PDZ domain–binding motif at the C-terminus of VE-cadherin involved in Par3 binding (Iden *et al.*, 2006; Tyler *et al.*, 2010). To test whether Par3 mediates Pals1 binding to VE-cadherin, we coexpressed VE-cadherin and Pals1 in Par3-depleted HEK293T cells. The absence of Par3 did not impair recruitment of Pals1 by VE-cadherin to cell–cell contacts, excluding Par3 as mediator of the interaction between Pals1 and VE-cadherin (Supplemental Figure S1). To address whether VE-cadherin is required for the localization of Pals1 at intercellular junctions of endothelial cells, we analyzed the subcellular localization of Pals1 in endothelial cells depleted of VE-cadherin. In control small interfering RNA (siRNA)–transfected cells, Pals1 appeared as thin signal lining the intercellular junctions (Figure 2C). In VE-cadherin–knockdown cells, Pals1 was reduced but still detectable at intercellular junctions, despite complete knockdown of VE-cadherin (Figure 2C, bottom). These observations indicate that VE-cadherin is not mandatory for Pals1 localization at intercellular junctions. Most likely, the presence of Pals1 at cell–cell junctions of VE-cadherin–depleted endothelial cells is due to the ability of Pals1 to interact with multiple binding partners at cell–cell junctions, including the cell polarity proteins CRB3, PATJ, and Par6 (Roh *et al.*, 2002; Hurd *et al.*, 2003; Makarova *et al.*, 2003; Wang *et al.*, 2004; Michel *et al.*, 2005).

### VE-cadherin regulates vascular lumen formation through Pals1 and Par3 binding

To address the functional relevance of the direct interactions between VE-cadherin and the two polarity proteins Pals1 and Par3, we replaced endogenous VE-cadherin in HUVECs with mutants of VE-cadherin that have lost the ability to directly interact with Pals1 or Par3. HUVECs were transduced simultaneously with virus particles encoding a short hairpin RNA (shRNA) directed against human VE-cadherin and virus particles encoding shRNA-insensitive murine VE-cadherin cDNA constructs containing mutations (VE-cad\_3A4) or deletions (VE-cad\_Δ5) in the binding regions for Pals1 or Par3, respectively. We first analyzed the knockdown efficiencies of endogenous VE-cadherin, as well as the levels of expression and subcellular localizations of the ectopic murine VE-cadherin constructs, by Western blot analyses and indirect immunofluorescence. Endogenous VE-cadherin

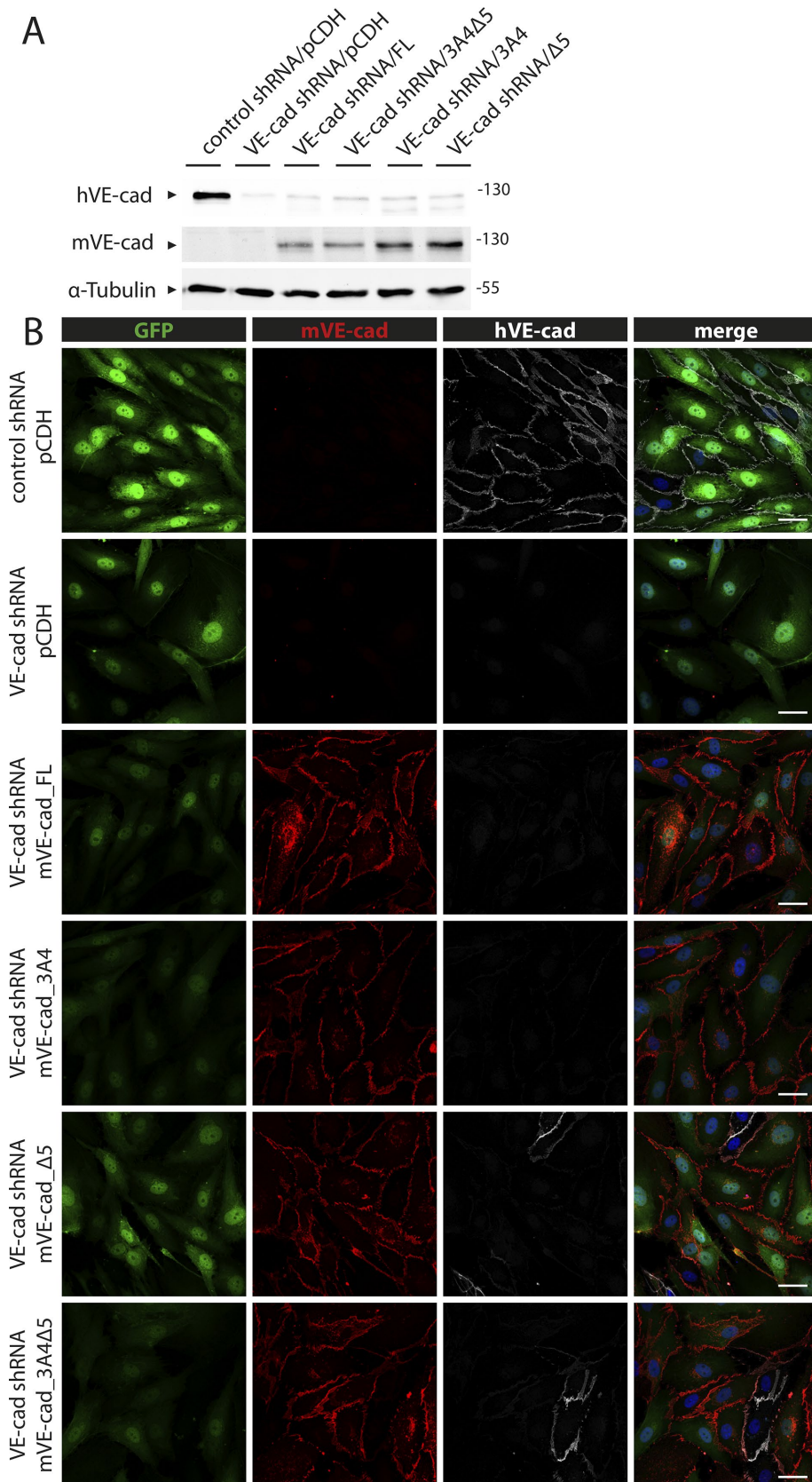


**FIGURE 3:** Replacement of endogenous VE-cadherin by VE-cadherin mutants lacking Pals1 and Par3 binding. (A) Western blot analysis of endogenous VE-cadherin and ectopically expressed mVE-cadherin (mVE-cad) or human VE-cadherin (hVE-cad) constructs in HUVECs. HUVECs were transduced with virus particles expressing either control shRNAs (control shRNA) or VE-cadherin-specific shRNAs (VE-cad shRNA) together with virus particles containing empty plasmid vectors (pCDH) or plasmid

was efficiently depleted in all cell populations generated (Figure 3, A and B). The overall expression levels of the ectopic VE-cadherin constructs were similar in all cell populations with slightly higher levels of the VE-cad\_3A4 and VE-cad\_Δ5 constructs than with the VE-cad\_FL and VE-cad/3A4\_Δ5 constructs (Figure 3A). All VE-cadherin constructs were specifically localized at interendothelial junctions (Figure 3B). In addition, the Pals-1 and Par3-binding mutant showed the same subcellular localization as VE-cadherin WT when ectopically expressed in highly polarizing MDCK cells grown on polycarbonate filters, that is, exclusive localization at intercellular junctions (Supplemental Figure S2). Finally, the mutations did not impair the adhesive activity of VE-cadherin, as analyzed by aggregation assays of transfected CHO cells (Supplemental Figure S3). These findings indicated that the introduced mutations did not affect the subcellular localization of VE-cadherin or change its adhesive activity.

We then analyzed lumen formation in a 3D collagen gel assay that mimics the process of vasculogenesis in vitro (Koh *et al.*, 2008). Lentivirally transduced HUVECs were mixed with collagen type I at 4°C and then transferred to 37°C to allow solidification of the collagen and subsequently grown for 48 h. Phase contrast images indicated that HUVECs developed lumen-containing spheroids under these conditions (Figure 4A, left). Lumen formation was confirmed by 3D reconstruction of confocal sections (Supplemental Movie S1). We next analyzed spheroid and lumen size by using

vectors encoding shRNA-insensitive mouse VE-cadherin constructs, including full-length VE-cadherin (FL), the Pals1/Par3 binding mutant of VE-cadherin (3A4Δ5), the Pals1 binding mutant of VE-cadherin (3A4), or the Par3 binding mutant of VE-cadherin (Δ5). Lysates derived from the different cell populations were analyzed with antibodies specific for human VE-cadherin (top) and mouse VE-cadherin (middle).  $\alpha$ -Tubulin served as loading control (bottom). (B) Localization of endogenous VE-cadherin and ectopically expressed mouse VE-cadherin (mVE-cad) constructs in HUVECs. HUVECs transduced with lentivirus particles as described in A were analyzed by immunofluorescence. Transduced cells were visualized by the GFP fluorescence signal, and ectopically expressed proteins were detected with antibodies specific for murine VE-cadherin (mVE-cad) or human VE-cadherin (hVE-cad). Note that all mVE-cadherin constructs localize to cell-cell contacts. Scale bar, 20  $\mu$ m.

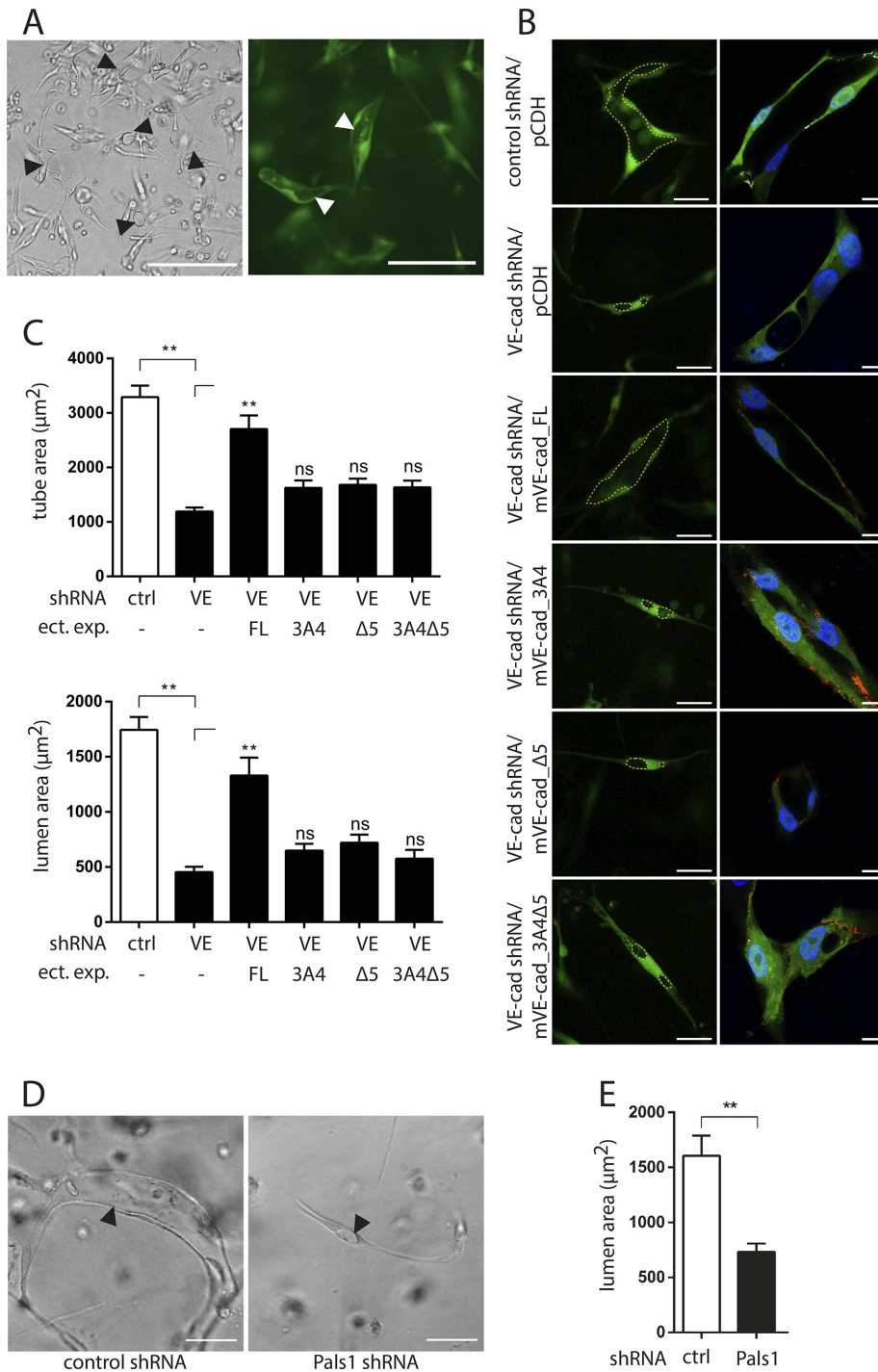


**FIGURE 4:** Spheroid formation of endothelial cells expressing Pals1 and Par3 binding mutants of VE-cadherin. (A) Spheroid formation of HUVECs grown in collagen. HUVECs transduced with GFP-encoding lentiviral control plasmids were grown for 48 h in 3D collagen gels and analyzed by phase contrast microscopy (left) or epifluorescence microscopy (right). Arrowheads point to lumen of spheroids. Scale bars, 200  $\mu\text{m}$ . (B) Representative epifluorescence and confocal micrographs of spheroids developed from HUVECs transduced with VE-cadherin shRNA and mVE-cadherin cDNA constructs as indicated. For confocal imaging, spheroids were analyzed for shRNA plasmid transduction (either control shRNA or hVE-cadherin shRNA; GFP fluorescence), localization of endogenous VE-cadherin (white signal), localization of ectopically expressed mouse VE-cadherin constructs (red signal), and DNA (blue signal). Scale bars, 50  $\mu\text{m}$  (epifluorescence images), 10  $\mu\text{m}$  (confocal images). (C) Statistical evaluation of spheroid formation of HUVECs transduced with VE-cadherin shRNA and mVE-cadherin cDNA constructs as indicated. Top, spheroid size as analyzed by the area of the spheroid. Bottom, lumen/vacuole size as analyzed by the area of the lumens/vacuoles. Quantitation of data shown here was

the GFP fluorescence signal resulting from the lentiviral transduction (Figure 4A, right). Cross-sections of spheroids were used to analyze the spheroid and lumen size. Control cells developed into spheroids that commonly consisted of three or more cells with a cross-sectional area of  $\sim 3200 \mu\text{m}^2$  and a cross-sectional lumen area of  $\sim 1700 \mu\text{m}^2$  (Figure 4, B and C). Confocal microscopy analysis indicated that the cells developed 3D spheroids consisting of a single lumen surrounded by two or three endothelial cells with a thin cytoplasm (Figure 4B), which is similar to what was observed previously (Davis and Camarillo, 1996; Lampugnani *et al.*, 2010). VE-cadherin depletion resulted in a dramatic reduction of cross-sectional spheroid and lumen size. In addition, the cells frequently contained intracellular vacuoles indicative for early stages of lumen formation (Kamei *et al.*, 2006; Lampugnani *et al.*, 2010; Wang *et al.*, 2010; Figure 4B, VE-cad shRNA). Ectopic expression of mVE-cadherin in VE-cadherin-depleted HUVECs restored spheroid and lumen size and also the ability of cells to develop multicellular spheroids with a single lumen (Figure 4, B and C, mVE-cad\_FL). Ectopic expression of the Pals1-binding mutant of VE-cadherin resulted in spheroids that were similar to spheroids originating from VE-cadherin-depleted cells. Both cross-sectional spheroid and lumen areas were not significantly larger than in VE-cadherin-knockdown spheroids (Figure 4, B and C, VE-cad\_3A4). In addition, instead of a single lumen, the spheroids frequently contained multiple small lumens or vacuoles, and the cytoplasm of the cells was enlarged compared with the thin cytoplasm

performed by one-way ANOVA followed by Dunnett's test. Data are derived from four independent experiments with 15 spheroids analyzed for each condition in each experiment. Data are presented as mean  $\pm$  SEM. ns, not significant,  $**p < 0.0001$ . (D) Spheroid formation of HUVECs after Pals1 depletion. Representative bright-field microscopy images of spheroids developed from control shRNA-transduced HUVECs (left) and Pals1 shRNA-transduced HUVECs (right). Scale bars, 50  $\mu\text{m}$ . (E) Statistical evaluation of lumen/vacuole size after Pals1 depletion as analyzed by the area of the lumens/vacuoles. Quantitation of data shown here was performed by one-way ANOVA followed by Dunnett's test. Data are derived from three independent experiments with a minimum of 15 spheroids analyzed for each condition in each experiment. Data are presented as means  $\pm$  SEM. ns, not significant,  $**p < 0.0001$ .

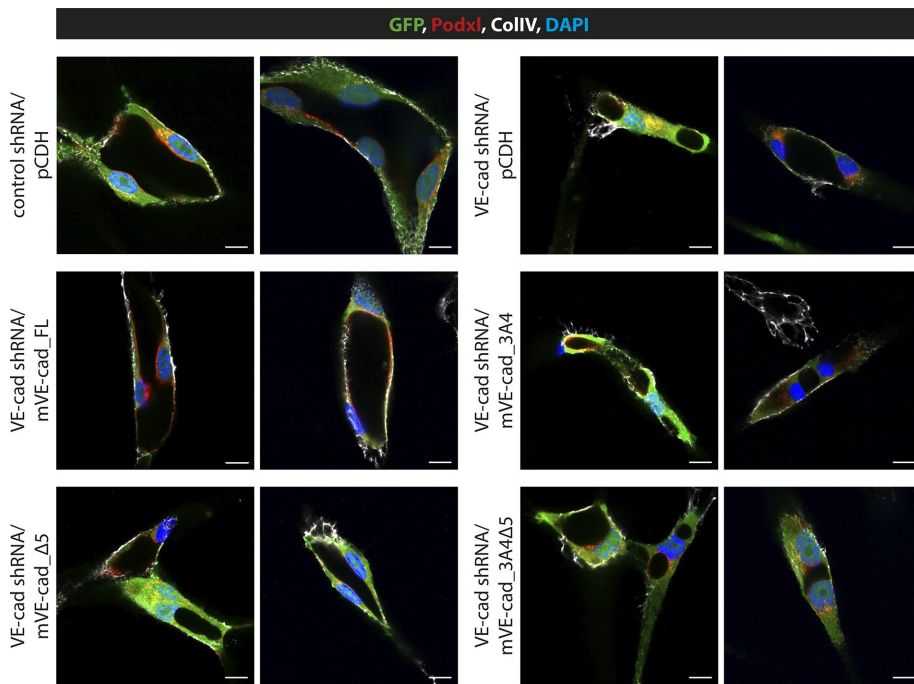


**FIGURE 5:** Membrane polarity of 3D-grown endothelial cells expressing Pals1 and Par3 binding mutants of VE-cadherin. HUVECs with endogenous VE-cadherin replaced by Pals1 or Par3 or Pals1/Par3 binding mutants were grown for 48 h in 3D collagen gels. Spheroids were stained with antibodies against podocalyxin (Podxl) and collagen type IV (Col IV) to stain the apical and basal membrane domains, respectively. Lentivirally transduced cells are visualized by GFP fluorescence, and nuclei are visualized with DAPI. Representative confocal images of HUVEC spheroids are shown for each construct. Scale bars, 10  $\mu$ m.

of mVE-cad\_FL-expressing VE-cadherin-knockdown endothelial cells (Figure 4, B and C; compare VE-cad\_FL and VE-cad\_3A4; Supplemental Movies S2 and S3). Similar to the Pals1 binding mutant, the Par3 binding mutant of VE-cadherin was unable to reestablish cross-sectional spheroid and lumen areas, and the spheroids contained intracellular vacuoles instead of a single lumen (Figure 4, B and C, VE-cad\_Δ5). Ectopic expression of a VE-cadherin mutant deficient for both Pals1 and Par3 binding resulted in spheroids that resembled those obtained after reexpression of the individual binding mutants alone, that is, spheroids with reduced cross-sectional spheroid and lumen areas and either multiple lumens or vacuoles surrounded by cells with highly enlarged cytoplasm (Figure 4, B and C, VE-cad\_3A4Δ5). The effects of the different VE-cadherin mutant constructs on spheroid size and lumen size are quantified in Figure 4C. Together these findings indicate that both the Pals1-binding motif in the JMD of VE-cadherin and the Par3-binding motif at the C-terminus of the CBD of VE-cadherin are required for normal spheroid development and lumen formation.

To directly analyze Pals1 function in spheroid development and lumen formation, we performed spheroid assays with Pals1-depleted HUVECs. Surprisingly, loss of Pals1 expression resulted in a drastically reduced number of spheroids (Supplemental Figure S4), suggesting a potential role of Pals1 in endothelial cell proliferation or survival, which was previously observed in neural progenitor cells (Kim *et al.*, 2010; Park *et al.*, 2016). Spheroids that developed from Pals1-knockdown cells had significantly smaller lumens than control cells (Figure 4D and Supplemental Figure S4), which is similar to what we observed in VE-cadherin-knockdown cysts. These findings indicate that Pals1 regulates spheroid development and suggest that this function is mediated through differ-

ent mechanisms, including cell proliferation, cell survival, and cell polarization.

### VE-cadherin regulates endothelial membrane polarity through Pals1 and Par3

We next analyzed membrane polarity in spheroids originating from control HUVECs, VE-cadherin-knockdown HUVECs, or HUVECs with endogenous VE-cadherin replaced by Pals1, Par3, or Pals1/Par3 binding mutants of VE-cadherin. Control cells developed regular spheroids with a central lumen in which the apical membrane marker podocalyxin (Podxl) was enriched along the apical membrane above the nucleus (Figure 5). The basal marker collagen IV (Coll IV) was restricted to the basal surface of the cells, where it was evenly distributed, similar to previous results (Lampugnani *et al.*, 2010). Depletion of VE-cadherin resulted in much smaller spheroids in which the polar distribution of Podxl and Coll IV was disturbed (Figure 5). Podxl was enriched at specific sites along intracellular vacuoles and absent at others. Similarly, Coll IV was unevenly distributed along the basal membrane domain. Ectopic expression of murine VE-cadherin completely restored this polarity defect induced by depletion of endogenous VE-cadherin. Of importance, neither the Pals-1 binding mutant nor the Par3 binding mutant

of VE-cadherin restored Podxl membrane polarity when expressed in VE-cadherin-depleted endothelial cells. In both VE-cadherin\_3A4- and VE-cadherin\_Δ5-reconstituted cells, Podxl was enriched at specific sites within vacuoles (Figure 5). The localization of Coll IV was less severely affected than Podxl, as the protein was still restricted to the basal membrane domain facing the collagen matrix. The phenotype of the VE-cadherin\_3A4Δ5-reconstituted spheroids was similar to the phenotypes seen for cells expressing the single mutants, that is, ectopic localization of Podxl at intracellular vacuoles but mostly basal localization of Coll IV (Figure 5). Together these observations indicate that VE-cadherin regulates apical membrane specification and vascular lumen formation through its interaction with both Pals1 and Par3.

### DISCUSSION

In this study, we identify the conserved cell polarity protein Pals1 as a novel binding partner of VE-cadherin. The interaction is direct and involves a membrane-proximal region in the cytoplasmic domain of VE-cadherin. We find that both the direct interaction with Pals1 and the previously identified interaction with Par3 are critical for the ability of VE-cadherin to regulate apicobasal polarity and vascular lumen formation. Our study identifies the two conserved cell polarity proteins Pals1 and Par3 as mediators of VE-cadherin-regulated polarity in vascular endothelial cells.

Of interest, although VE-cadherin serves as an interaction partner of Pals1, we found that both after depletion of VE-cadherin in endothelial cells and upon ectopic expression of the Pals1 binding mutant of VE-cadherin in HEK293T cells, Pals1 can still localize at cell-cell contacts. The cell-cell contact localization in VE-cadherin-knockdown endothelial cells can most likely be explained by the multiple

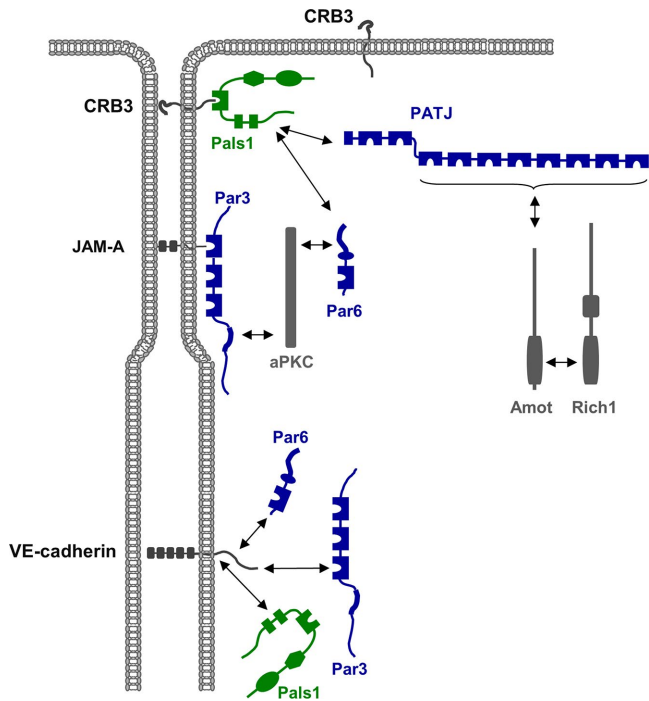


**FIGURE 6:** The Pals1 interaction network. Pals1 directly interacts with several scaffolding proteins localized at tight junctions and adherens junctions, including PATJ and Par6. In addition, Pals1 directly interacts with transmembrane proteins CRB3 and VE-cadherin. Direct interactions are indicated by double arrows. Note that the interactions of Pals1 with CRB3, Par6, and PATJ have been demonstrated in epithelial cells, and the interaction with VE-cadherin is specific for endothelial cells.

protein interactions that have been described for Pals1. In epithelial cells, Pals1 is part of the CRB3-Pals1-PATJ complex and interacts directly with both CRB3 and PATJ (Roh *et al.*, 2002; Michel *et al.*, 2005; Figure 6), which is one possible mechanism for Pals1 localization in the absence of VE-cadherin. Furthermore, PATJ can interact with other transmembrane proteins, including JAM-A and Nectin-1 (Adachi *et al.*, 2009), providing a second possible mechanism for Pals1 localization in the absence of VE-cadherin. The normal recruitment of Pals1 in HEK293T cells expressing the VE-cadherin/3A4 mutant but not with the VE-cadherin PDZ domain-binding mutant (VE-cadherin/ $\Delta$ 5) could also be explained by an indirect association of Pals1 with VE-cadherin through a PDZ domain protein interacting with VE-cadherin. Par3 would be likely candidate, since it can interact with the Pals1 binding partner Par6 (Hurd *et al.*, 2003; Wang *et al.*, 2004). However, we can rule out Par3 as mediator of this interaction because the absence of Par3 did not affect Pals1 recruitment in transfected HEK293T cells (Supplemental Figure S1).

Our studies further emphasize an important role for VE-cadherin in vascular lumen formation and identify two molecular binding partners through which VE-cadherin mediates this activity, namely Pals1 and Par3. According to the current model, *de novo* lumen formation is initiated when two apposing cells in endothelial cell cords form close cell-cell contacts via VE-cadherin trans-homophilic interactions (Zeeb *et al.*, 2010). VE-cadherin recruits the sialomucins CD34 and Podxl to the site of cell-cell contact, thereby initiating the separation of the two contacting cell membranes by way of repulsive forces mediated by the negatively charged carbohydrates on sialomucins (Strilic *et al.*, 2009, 2010). Localization of CD34 and Podxl at the cell-cell contact site is followed by the recruitment of moesin, which stabi-

lizes F-actin at the newly formed apical membrane. Vascular endothelial growth factor (VEGF) signaling triggers the interaction of nonmuscle myosin II with F-actin and actomyosin-driven cell shape changes that are required for lumen formation (Zeeb *et al.*, 2010). The further steps after these primary events are less well understood. The initiation of apical membrane specification driven by VE-cadherin-mediated cell adhesion must be reinforced and propagated in order to maintain apicobasal membrane polarity, as described in epithelial cells (Yeaman *et al.*, 1999). We hypothesize that VE-cadherin contributes to the maintenance of apicobasal membrane polarity and stable lumen formation via both polarity proteins, Pals1 and Par3.

The interaction with Pals1 probably serves to stabilize F-actin at the apical membrane. In parietal epithelial cells, Pals1 interacts with ezrin, a member of the ezrin-radixin-moesin (ERM) family, and regulates Ezrin recruitment to the apical membrane domain, which is required for the remodeling of the apical membrane cytoskeleton associated with vectorial secretion (Cao *et al.*, 2005). In MDCK epithelial cells, a complex consisting of Podxl, NHERF1, and ezrin promotes apical membrane identity, most likely through the activity of phosphorylated ezrin to stabilize the localization of a NHERF1-Podxl complex at the apical membrane (Bryant *et al.*, 2014). The ERM-family protein predominantly expressed in endothelial cells is moesin (Fehon *et al.*, 2010). Thus, by recruiting moesin through Pals1 to cell-cell junctions VE-cadherin most likely contributes to the formation of the apical membrane. In agreement with this, VE-cadherin and moesin1 are required for the establishment and maintenance of apicobasal polarity during lumen formation in the intersegmental vessels of the zebrafish embryo (Wang *et al.*, 2010). Of note, Pals1 was recently shown to be involved in the regulation of cell cycle progression and cell survival of neural progenitor cells in the cerebrum and cerebellum, which is in part mediated by an influence on the mammalian target of rapamycin (mTOR) signaling pathway (Kim *et al.*, 2010; Park *et al.*, 2016). Our observation of a strongly reduced number of spheroids after Pals1 depletion in HUVECs (Supplemental Figure S4) is in line with a similar role of Pals1 in endothelial cells. Thus we speculate that Pals1 contributes to vascular lumen formation not only by regulating apical membrane identity, but also by maintaining endothelial cells in a proliferative and antiapoptotic state. The impaired spheroid formation in cells expressing the Pals1 binding-defective mutant of VE-cadherin (Figure 4, B and C) could then in part be explained by putative mislocalization of Pals1 resulting in altered or defective mTOR signaling and reduced cell survival.

The interaction of VE-cadherin with Par3 probably contributes to the development of apical membrane identity. Par3 interacts with various phosphoinositides, including phosphatidylinositol 4,5-bisphosphate (PtdIns(4,5)P<sub>2</sub>) and phosphatidylinositol-3,4,5-trisphosphate (PtdIns(3,4,5)P<sub>3</sub>), and with the lipid phosphatase Phosphatase and Tensin Homologue (PTEN; Wu *et al.*, 2007). In polarized epithelial cells, PtdIns(4,5)P<sub>2</sub> is localized at the apical membrane, whereas PtdIns(3,4,5)P<sub>3</sub> is localized at the basolateral membrane but excluded from the apical membrane (Gassama-Diagne *et al.*, 2006). The apical segregation of phosphoinositides is regulated by apically localized PTEN (Martin-Belmonte *et al.*, 2007), which confers apical membrane identity by dephosphorylating apical PtdIns(3,4,5)P<sub>3</sub> to PtdIns(4,5)P<sub>2</sub>. Intriguingly, loss of PTEN function in MDCK cells and loss of apical localization of a Par3-aPKC complex during mouse mammary epithelium development inhibit lumen formation and ductal morphogenesis, respectively (Martin-Belmonte *et al.*, 2007; Elias *et al.*, 2015). Thus, by recruiting PTEN through Par3, VE-cadherin probably contributes to the specification of apical and basolateral membranes as a prerequisite for lumen formation.

One important observation of our study is that the lack of direct binding of Pals1 and Par3 to VE-cadherin results in a phenotype comparable to the complete lack of VE-cadherin expression, that is, disorganized spheroids that contain one or several large vacuoles (Figures 4 and 5; Supplemental Movies S1 and S2). The formation of the vascular lumen has been proposed to be regulated either by fusion of intracellular vesicles and vacuoles, which coalesce with vacuoles from neighboring cells (cell hollowing), or selective recruitment of apical membrane determinants to sites of cell–cell contacts at early stages of lumenization followed by membrane separation and cell–cell contact segregation (cord hollowing; Iruela-Arispe and Davis, 2009; Neufeld *et al.*, 2014). It is likely that both mechanisms contribute to tube formation, and the relative contributions of the two mechanisms might depend on the type of blood vessel and vascular bed (Wang *et al.*, 2010). In addition, vacuoles not only fuse and coalesce with vacuoles from adjacent cells, but they can also fuse with the luminal membrane and thereby contribute to lumen expansion during the cord-hollowing mechanism of lumenization (Wang *et al.*, 2010; Zovein *et al.*, 2010). Of interest, lack of  $\beta$ 1-integrin in nascent endothelial cells results in reduced expression of Par3 and mislocalization of VE-cadherin, concomitant with abnormal accumulation of intracellular vacuoles, which most likely fail to fuse with the nascent apical membrane as a result of disturbed membrane polarity (Zovein *et al.*, 2010; Yamamoto *et al.*, 2015). Together with these published findings, our observations suggest that VE-cadherin interacts with the two cell polarity regulators Pals1 and Par3 downstream of  $\beta$ 1-integrin to regulate apical membrane specification and luminal vesicle fusion during lumen morphogenesis.

## MATERIALS AND METHODS

### Cell culture and transfections

HUVECs were obtained from PromoCell (Heidelberg, Germany; C-12203) and maintained in Endothelial Growth Medium 2 (C-22011; PromoCell) as recommended by the manufacturer. HEK293T and MDCKII cells (Sigma-Aldrich, Munich, Germany) were maintained in DMEM (Sigma-Aldrich) supplemented with 10% fetal calf serum (FCS), 2 mM glutamine, and 100 U/ml penicillin/streptomycin. VE-cadherin–transfected CHO cells (Iden *et al.*, 2006) were maintained in  $\alpha$ -MEM (Biochrom, Berlin, Germany) supplemented with 10% FCS, 2 mM glutamine, 100 U/ml penicillin/streptomycin and 500  $\mu$ g/ml G418. Transient transfections of plasmids in HEK293T, MDCKII cells, and CHO cells were performed using either Xfect Transfection Reagent (Clontech Laboratories, Mountain View, CA) or Lipofectamine 2000 Transfection Reagent (Life Technologies, Darmstadt, Germany) according to the manufacturer's instructions. siRNA oligonucleotide transfections of HUVECs were performed using Xfect Transfection Reagent according to the manufacturer's instructions. shRNA-encoding plasmids and cDNA plasmids encoding various murine VE-cadherin constructs were introduced into HUVECs by lentiviral transduction. Lentiviral particles were produced in HEK293T cells by cotransfection of the lentiviral vectors pLVTHM (Addgene plasmid 12247) or pCDH-CMV-MCS-EF1-Puro (System Biosciences, Mountain View, CA) with the packaging vectors psPAX2 (Addgene plasmid 12260) and pMD2.G (Addgene plasmid 12259) in a ratio of 4:3:1. The next day, HEK293T culture medium was replaced by Endothelial Growth Medium 2, and after 24 h of incubation, lentivirus particle–containing HEK293T supernatants were transferred to HUVECs. After overnight incubation with lentivirus particles, the cells were cultured for an additional 2 d in the absence of virus particles before analysis.

### Antibodies and reagents

The following antibodies were used: goat polyclonal antibody (pAb) anti-VE-cadherin (sc-6458; Santa Cruz Biotechnology, Dallas, TX), mouse monoclonal antibody (mAb) anti-VE-cadherin (610252; BD Biosciences, Heidelberg, Germany), rat mAb anti-VE-cadherin 11D4.1 (550548; BD Biosciences), mouse mAb anti-Flag tag (F1804; Sigma-Aldrich), rabbit pAb anti-Flag tag (F7425; Sigma-Aldrich), rabbit pAb anti-ZO1 (61-7300; Thermo Fisher Scientific, Waltham, MA), rabbit pAb anti-MPP5/Pals1 (HPA000993; Sigma-Aldrich), mouse mAb anti- $\alpha$ -tubulin (T5168; Sigma-Aldrich), goat pAb anti-podocalyxin (AF1658; R&D Systems, Minneapolis, MN), rabbit pAb anti-collagen IV (2150-0140; AbD Serotec, Puchheim, Germany), and rabbit pAb anti-Par3 (Iden *et al.*, 2006). We used basic fibroblast growth factor (bFGF; Peprotech, Hamburg, Germany) and VEGF (Peprotech) as reagents.

### RNA interference

To deplete VE-cadherin in HUVECs, we used the siRNA oligonucleotide 5'-AGAUGCAGAGGCUCAUGAUTT-3' (Schafer *et al.*, 2003). As control siRNA, we used a nontargeting siRNA (On-TARGETplus Non-targeting siRNA; Thermo Fisher Scientific). For lentiviral downregulation of VE-cadherin in HUVECs, the oligonucleotides 5'-CGC-GTCCCCAGATGCAGAGGCTCATGATTTCAAGAGAATCATGAGCCTCTGCATCTTTTTGGAAAT-3' and 5'-CGATTTCCAAA-AAGATGCAGAGGCTCATGATTCTTTGAAATCATGAGCCTCTGCATCTGGGGA-3' were annealed and cloned into the shRNA expression vector pLVTHM. As negative control, the oligonucleotides 5'-CGCGTCCCCGGCAGCACAACACTGCATTGTT CAAGAGACAA-GTGCAGTTGTGCTGCCTTTTTGGAAAT-3' and 5'-CGATTTCCAAA-AAGGCAGCACAACACTGCATTGTCTCTTGAACAAGTGCAGTTGTGCGCCGGGGA-3' were annealed and cloned into pLVTHM. These two oligos encode for a shRNA not targeting human VE-cadherin. Knockdown of Pals1 was performed using a commercially available pool of three Pals1-specific shRNA–encoding lentiviral vector plasmids (sc-43991-SH; Santa Cruz Biotechnology). Knockdown of Par3 was performed using a lentiviral shRNA plasmid targeting human PARD3 (RHS3979-201817648; Dharmacon).

### DNA constructs

The following GST-fusion constructs were described previously: murine VE-cadherin cytoplasmic domain lacking five amino acids (aa) at the C-terminal end (VE-cad/CP $\Delta$ 5, aa 621–784), murine E-cadherin cytoplasmic domain (E-cad/CP, aa 732–882), murine N-cadherin cytoplasmic domain (N-cad/CP, aa 747–906; Iden *et al.*, 2006). The following GST-fusion proteins, which contain specific subregions or mutations of the cytoplasmic domain of murine VE-cadherin, were generated in pGEX-4T-1: VE-cad/proximal (aa 621–689), VE-cad/middle (aa 661–730), VE-cad/distal (aa 714–784), VE-cad/3A1 (aa 621–689, aa 667–669 replaced by Ala), VE-cad/3A2 (aa 621–689, aa 670–672 replaced by Ala), VE-cad/3A3 (aa 621–689, aa 673–675 replaced by Ala), VE-cad/3A4 (aa 621–689, aa 621–623 replaced by Ala), and VE-cad/3A5 (aa 621–689, aa 624–626 replaced by Ala). The following expression constructs were cloned into pcDNA3 and pCDH-CMV-MCS-EF1-Puro: mVE-cad\_FL (murine full-length VE-cadherin), mVE-cad\_3A4 (aa 621–623 replaced by Ala), mVE-cad\_ $\Delta$ 5 (aa 780–784 deleted), and mVE-cad\_3A4 $\Delta$ 5 (aa 621–623 replaced by Ala and aa 780–784 deleted). Human Pals1 full-length cDNA was cloned into pcDNA3.1/nV5-Dest plasmid vector (Invitrogen, Carlsbad, CA) for in vitro transcription/translation, into pcDNA-DEST53 (Invitrogen) for ectopic expression of N-terminally GFP-tagged Pals1, and into pQCXIP-3xFlag for ectopic expression of N-terminally Flag-tagged Pals1.

## Immunoprecipitation and Western blot analysis

For immunoprecipitations, cells were lysed in lysis buffer (50 mM Tris HCl, pH 7.4, 1% [vol/vol] Nonidet P-40 [AppliChem, Darmstadt, Germany], 150 mM NaCl, and protease inhibitors [cOmplete Protease Inhibitor Cocktail; Roche, Indianapolis, IN]) for 30 min on ice and then centrifuged at 4°C. Postnuclear supernatants were incubated with 3 µg of antibodies coupled to protein A- or protein G-Sepharose beads (GE Healthcare, Solingen, Germany) overnight at 4°C. Immune complex-captured beads were washed five times with lysis buffer without inhibitors and boiled in SDS sample buffer containing 0.1 M dithiothreitol. The proteins were separated by SDS-PAGE and analyzed by Western blotting with near-infrared fluorescence detection (Odyssey imaging system and IRDye 800CW conjugated antibodies; LI-COR Biosciences, Bad Homburg, Germany).

## In vitro binding experiments

In vitro binding experiments were performed as described previously (Ebnet *et al.*, 2000). Briefly, GST-fusion proteins were expressed in *Escherichia coli* BL21 (GE Healthcare). Bacteria were lysed by passing through a French pressure cell, and GST-fusion proteins were purified by affinity chromatography. Protein solutions were adjusted to 50% (wt/vol) glycerol and stored at -20°C. For GST pull-down experiments, the prey proteins were generated in vitro using the TNT T7-coupled reticulocyte lysate system (Promega, Madison, WI) in the presence of <sup>35</sup>[S]methionine as described by the manufacturer. We incubated 10 µl of the translation reactions with 3 mg of GST-fusion proteins immobilized on glutathione-Sepharose 4B beads (Life Technologies) for 2 h at 4°C under constant agitation. Beads were washed five times with buffer B (10 mM 4-(2-hydroxyethyl)-1-piperazineethanesulfonic acid [HEPES], pH 7.2, 100 mM KCl, 1 mM MgCl<sub>2</sub>, 0.1% Triton X-100). Bound proteins were eluted by boiling for 5 min in SDS sample buffer, subjected to SDS-PAGE, and analyzed by fluorography.

## Immunofluorescence microscopy

Immunofluorescence analyses were performed with cells grown on fibronectin-coated chamber slides (Lab-Tek II; Thermo Fisher Scientific). Cells were fixed in either 4% paraformaldehyde for 10 min or ice-cold MetOH for 5 min. Paraformaldehyde-fixed cells were permeabilized for 10 min in phosphate-buffered saline (PBS) containing 0.5% Triton X-100 and subsequently washed with PBS containing 100 mM glycine for 10 min. Blocking was performed for 1 h at room temperature with blocking buffer (PBS, 10% FCS, 0.2% Triton X-100, 0.05% Tween 20, 0.02% BSA) followed by incubation with primary antibodies in blocking buffer overnight at 4°C. Incubation with secondary antibodies (Alexa Fluor 488-, 594-, and 647-conjugated, highly cross-adsorbed secondary antibodies; Life Technologies) and 1 µg/ml 4',6-diamidino-2-phenylindole (DAPI; Sigma-Aldrich) was performed in blocking buffer for 1 h at room temperature. Finally, samples were washed with blocking buffer and mounted in fluorescence mounting medium (Mowiol 4-88; Sigma-Aldrich). Immunofluorescence microscopy was performed using an LSM 780 confocal microscope (Carl Zeiss, Jena, Germany) equipped with Plan-Neofluar 20×/0.5 and Plan-Apochromat 63×/1.4 oil differential interference contrast objective lenses (Carl Zeiss). Phase contrast microscopy was performed using an EVOS Fluorescence Microscope (Advanced Microscopy Group, Mill Creek, WA). To quantify Pals1 localization in transfected HEK293T cells, the cell-cell contact area was defined as the area reaching 0.25 µm into each of the two contacting cells. The Pals1 intensity is given as ratio of the mean intensities measured at cell-cell contacts and in the cytoplasm of the contacting cells.

## Three-dimensional culture

HUVEC 3D cultures in collagen gels were performed as described (Bayless and Davis, 2002; Lampugnani *et al.*, 2010). Briefly, HUVECs were seeded at a concentration of  $5 \times 10^5$  cells/ml in 3.5 mg/ml collagen gels (collagen type I from rat tail, high concentration; BD Biosciences). For confocal immunofluorescence, analysis 200 µl of the cell suspension in collagen was added to each well of a µ-Slide 8 Well (ibidi, Martinsried, Germany). After incubation for 30 min at 37°C in a humidified CO<sub>2</sub> incubator, the collagen gel was overlaid with 200 µl of medium (M199 with 1% FCS, insulin-transferin-selenium supplement, 50 ng/ml phorbol myristate acetate, 50 µg/ml ascorbic acid, 40 ng/ml VEGF, and 40 ng/ml bFGF). HUVEC 3D cultures were cultivated for 48 h and then fixed and processed for immunofluorescence microscopy. Spheroids were fixed in 4% paraformaldehyde for 35 min and permeabilized in PBS containing 0.5% Triton X-100 for 20 min. Incubation with primary and secondary antibodies was performed overnight. Immunostained spheroids were analyzed by confocal microscopy as described. For spheroid and lumen size quantitation, 50 µl of the cell suspension in collagen was added per well of a 96-well microplate. Spheroid and lumen sizes were analyzed by taking cross-sectional images of randomly selected spheroids at 20× magnification. Areas were measured with ImageJ software (National Institutes of Health, Bethesda, MD).

## Cell aggregation assays

For aggregation assays, CHO cells transfected with VE-cadherin constructs were harvested, washed in Hanks balanced salt solution, 2 mM CaCl<sub>2</sub>, and 25 mM HEPES, and then counted and adjusted to  $1 \times 10^6$ /ml. A 3-ml amount of cell suspension was added to a 30-mm BSA-coated Petri dish and incubated on a horizontal shaker at 35 rpm for 45 min at 37°C. Cells were fixed by addition of 500 µl of 25% glutaraldehyde and incubation on ice for 30 min. The particles were counted using ImageJ software. Particles >256 µm<sup>2</sup> were considered as aggregates.

## Statistical analysis

Statistical analysis was performed using GraphPad Prism 6.0 (GraphPad Software, La Jolla, CA). Statistical significances in Figures 2B and 4C and Supplemental Figures S1 and S3 were calculated by one-way analysis of variance (ANOVA) with Dunnett's post hoc test.

## ACKNOWLEDGMENTS

We thank Frauke Brinkmann for expert technical assistance. This work was supported by grants from the Medical Faculty of the University of Münster (IZKF Eb2/028/09 and Eb2/020/14) and the Deutsche Forschungsgemeinschaft (Ge514/9-1).

## REFERENCES

- Adachi M, Hamazaki Y, Kobayashi Y, Itoh M, Tsukita S, Furuse M, Tsukita S (2009). Similar and distinct properties of MUPP1 and Patj, two homologous PDZ domain-containing tight-junction proteins. *Mol Cell Biol* 29, 2372–2389.
- Bayless KJ, Davis GE (2002). The Cdc42 and Rac1 GTPases are required for capillary lumen formation in three-dimensional extracellular matrices. *J Cell Sci* 115, 1123–1136.
- Bryant DM, Rognot J, Datta A, Overeem AW, Kim M, Yu W, Peng X, Eastburn DJ, Ewald AJ, Werb Z, *et al.* (2014). A molecular switch for the orientation of epithelial cell polarization. *Dev Cell* 31, 171–187.
- Cao X, Ding X, Guo Z, Zhou R, Wang F, Long F, Wu F, Bi F, Wang Q, Fan D, *et al.* (2005). PALS1 specifies the localization of ezrin to the apical membrane of gastric parietal cells. *J Biol Chem* 280, 13584–13592.
- Davis GE, Camarillo CW (1996). An alpha 2 beta 1 integrin-dependent pinocytotic mechanism involving intracellular vacuole formation and

- coalescence regulates capillary lumen and tube formation in three-dimensional collagen matrix. *Exp Cell Res* 224, 39–51.
- Dejana E (2004). Endothelial cell-cell junctions: happy together. *Nat Rev Mol Cell Biol* 5, 261–270.
- Dupre-Crochet S, Figueroa A, Hogan C, Ferber EC, Bialucha CU, Adams J, Richardson EC, Fujita Y (2007). Casein kinase 1 is a novel negative regulator of E-cadherin-based cell-cell contacts. *Mol Cell Biol* 27, 3804–3816.
- Ebnet K, Schulz CU, Meyer Zu Brickwedde MK, Pendl GG, Vestweber D (2000). Junctional adhesion molecule interacts with the PDZ domain-containing proteins AF-6 and ZO-1. *J Biol Chem* 275, 27979–27988.
- Elias S, McGuire JR, Yu H, Humbert S (2015). Huntingtin is required for epithelial polarity through RAB11A-mediated apical trafficking of PAR3-aPKC. *PLoS Biol* 13, e1002142.
- Fehon RG, McClatchey AI, Bretscher A (2010). Organizing the cell cortex: the role of ERM proteins. *Nat Rev Mol Cell Biol* 11, 276–287.
- Funke L, Dakoji S, Bredt DS (2005). Membrane-associated guanylate kinases regulate adhesion and plasticity at cell junctions. *Annu Rev Biochem* 74, 219–245.
- Gassama-Diagne A, Yu W, ter Beest M, Martin-Belmonte F, Kierbel A, Engel J, Mostov K (2006). Phosphatidylinositol-3,4,5-trisphosphate regulates the formation of the basolateral plasma membrane in epithelial cells. *Nat Cell Biol* 8, 963–970.
- Hurd TW, Gao L, Roh MH, Macara IG, Margolis B (2003). Direct interaction of two polarity complexes implicated in epithelial tight junction assembly. *Nat Cell Biol* 5, 137–142.
- Iden S, Rehder D, August B, Suzuki A, Wolburg-Buchholz K, Wolburg H, Ohno S, Behrens J, Vestweber D, Ebnet K (2006). A distinct PAR complex associates physically with VE-cadherin in vertebrate endothelial cells. *EMBO Rep* 7, 1239–1246.
- Iruela-Arispe ML, Davis GE (2009). Cellular and molecular mechanisms of vascular lumen formation. *Dev Cell* 16, 222–231.
- Kamei M, Saunders WB, Bayless KJ, Dye L, Davis GE, Weinstein BM (2006). Endothelial tubes assemble from intracellular vacuoles in vivo. *Nature* 442, 453–456.
- Kim S, Lehtinen MK, Sessa A, Zappaterra MW, Cho SH, Gonzalez D, Boggan B, Austin CA, Wijnholds J, Gambello MJ, et al. (2010). The apical complex couples cell fate and cell survival to cerebral cortical development. *Neuron* 66, 69–84.
- Koh W, Stratman AN, Sacharidou A, Davis GE (2008). In vitro three dimensional collagen matrix models of endothelial lumen formation during vasculogenesis and angiogenesis. *Methods Enzymol* 443, 83–101.
- Lampugnani MG, Orsenigo F, Rudini N, Maddaluno L, Boulday G, Chapon F, Dejana E (2010). CCM1 regulates vascular-lumen organization by inducing endothelial polarity. *J Cell Sci* 123, 1073–1080.
- Lampugnani MG, Zanetti A, Breviaro F, Balconi G, Orsenigo F, Corada M, Spagnuolo R, Betson M, Braga V, Dejana E (2002). VE-cadherin regulates endothelial actin activating Rac and increasing membrane association of Tiam. *Mol Biol Cell* 13, 1175–1189.
- Liu Y, Collins C, Kiosses WB, Murray AM, Joshi M, Shepherd TR, Fuentes EJ, Tzima E (2013). A novel pathway spatiotemporally activates Rac1 and redox signaling in response to fluid shear stress. *J Cell Biol* 201, 863–873.
- Lubarsky B, Krasnow MA (2003). Tube morphogenesis: making and shaping biological tubes. *Cell* 112, 19–28.
- Macara IG (2004). Parsing the polarity code. *Nat Rev Mol Cell Biol* 5, 220–231.
- Makarova O, Roh MH, Liu CJ, Laurinec S, Margolis B (2003). Mammalian Crumbs3 is a small transmembrane protein linked to protein associated with Lin-7 (Pals1). *Gene* 302, 21–29.
- Martin-Belmonte F, Gassama A, Datta A, Yu W, Rescher U, Gerke V, Mostov K (2007). PTEN-mediated apical segregation of phosphoinositides controls epithelial morphogenesis through Cdc42. *Cell* 128, 383–397.
- Martin-Belmonte F, Yu W, Rodriguez-Fraticelli AE, Ewald AJ, Werb Z, Alonso MA, Mostov K (2008). Cell-polarity dynamics controls the mechanism of lumen formation in epithelial morphogenesis. *Curr Biol* 18, 507–513.
- McCaffrey LM, Macara IG (2011). Epithelial organization, cell polarity, and tumorigenesis. *Trends Cell Biol* 21, 727–735.
- Michel D, Arsanto JP, Massey-Harroche D, Beclin C, Wijnholds J, Le Bivic A (2005). PATJ connects and stabilizes apical and lateral components of tight junctions in human intestinal cells. *J Cell Sci* 118, 4049–4057.
- Neufeld S, Planas-Paz L, Lammert E (2014). Blood and lymphatic vascular tube formation in mouse. *Semin Cell Dev Biol* 31, 115–123.
- Park JY, Hughes LJ, Moon UY, Park R, Kim SB, Tran K, Lee JS, Cho SH, Kim S (2016). The apical complex protein Pals1 is required to maintain cerebellar progenitor cells in a proliferative state. *Development* 143, 133–146.
- Rodriguez-Boulan E, Macara IG (2014). Organization and execution of the epithelial polarity programme. *Nat Rev Mol Cell Biol* 15, 225–242.
- Roh MH, Fan S, Liu CJ, Margolis B (2003). The Crumbs3-Pals1 complex participates in the establishment of polarity in mammalian epithelial cells. *J Cell Sci* 116, 2895–2906.
- Roh MH, Makarova O, Liu CJ, Shin K, Lee S, Laurinec S, Goyal M, Wiggins R, Margolis B (2002). The Maguk protein Pals1, functions as an adapter, linking mammalian homologues of Crumbs and Discs Lost. *J Cell Biol* 157, 161–172.
- Ruffer C, Strey A, Janning A, Kim KS, Gerke V (2004). Cell-cell junctions of dermal microvascular endothelial cells contain tight and adherens junction proteins in spatial proximity. *Biochemistry* 43, 5360–5369.
- Schafer R, Abraham D, Paulus P, Blumer R, Grimm M, Wojta J, Aharinejad S (2003). Impaired VE-cadherin/beta-catenin expression mediates endothelial cell degeneration in dilated cardiomyopathy. *Circulation* 108, 1585–1591.
- Schulze C, Firth JA (1993). Immunohistochemical localization of adherens junction components in blood-brain barrier microvessels of the rat. *J Cell Sci* 104, 773–782.
- Simionescu M, Simionescu N, Palade GE (1975). Segmental differentiations of cell junctions in the vascular endothelium. *The microvasculature. J Cell Biol* 67, 863–885.
- Simionescu M, Simionescu N, Palade GE (1976). Segmental differentiations of cell junctions in the vascular endothelium. *Arteries and veins. J Cell Biol* 68, 705–723.
- Straight SW, Shin K, Fogg VC, Fan S, Liu CJ, Roh M, Margolis B (2004). Loss of PALS1 expression leads to tight junction and polarity defects. *Mol Biol Cell* 15, 1981–1990.
- Strilic B, Eglinger J, Krieg M, Zeeb M, Axnick J, Babal P, Muller DJ, Lammert E (2010). Electrostatic cell-surface repulsion initiates lumen formation in developing blood vessels. *Curr Biol* 20, 2003–2009.
- Strilic B, Kucera T, Eglinger J, Hughes MR, McNagny KM, Tsukita S, Dejana E, Ferrara N, Lammert E (2009). The molecular basis of vascular lumen formation in the developing mouse aorta. *Dev Cell* 17, 505–515.
- Suzuki S, Sano K, Tanihara H (1991). Diversity of the cadherin family: evidence for eight new cadherins in nervous tissue. *Cell Regul* 2, 261–270.
- Tanihara H, Sano K, Heimark RL, St John T, Suzuki S (1994). Cloning of five human cadherins clarifies characteristic features of cadherin extracellular domain and provides further evidence for two structurally different types of cadherin. *Cell Adhes Commun* 2, 15–26.
- Tyler RC, Peterson FC, Volkman BF (2010). Distal interactions within the par3-VE-cadherin complex. *Biochemistry* 49, 951–957.
- Vincent PA, Xiao K, Buckley KM, Kowalczyk AP (2004). VE-cadherin: adhesion at arm's length. *American journal of physiology. Cell Physiol* 286, C987–C997.
- Vorbrodt AW, Dobrogowska DH (2003). Molecular anatomy of intercellular junctions in brain endothelial and epithelial barriers: electron microscopist's view. *Brain Res Brain Res Rev* 42, 221–242.
- Wang Q, Hurd TW, Margolis B (2004). Tight junction protein Par6 interacts with an evolutionarily conserved region in the amino terminus of PALS1/Stardust. *J Biol Chem* 279, 30715–30721.
- Wang Y, Kaiser MS, Larson JD, Nasevicius A, Clark KJ, Wadman SA, Roberg-Perez SE, Ekker SC, Hackett PB, McGrail M, et al. (2010). Moesin1 and Ve-cadherin are required in endothelial cells during in vivo tubulogenesis. *Development* 137, 3119–3128.
- Wu H, Feng W, Chen J, Chan LN, Huang S, Zhang M (2007). PDZ domains of Par-3 as potential phosphoinositide signaling integrators. *Mol Cell* 28, 886–898.
- Yamamoto H, Ehling M, Kato K, Kanai K, van Lessen M, Frye M, Zeuschner D, Nakayama M, Vestweber D, Adams RH (2015). Integrin beta1 controls VE-cadherin localization and blood vessel stability. *Nat Commun* 6, 6429.
- Yeaman C, Grindstaff KK, Nelson WJ (1999). New perspectives on mechanisms involved in generating epithelial cell polarity. *Physiol Rev* 79, 73–98.
- Zeeb M, Strilic B, Lammert E (2010). Resolving cell-cell junctions: lumen formation in blood vessels. *Curr Opin Cell Biol* 22, 626–632.
- Zegers MM, O'Brien LE, Yu W, Datta A, Mostov KE (2003). Epithelial polarity and tubulogenesis in vitro. *Trends Cell Biol* 13, 169–176.
- Zovein AC, Luque A, Turlo KA, Hofmann JJ, Yee KM, Becker MS, Fassler R, Mellman I, Lane TF, Iruela-Arispe ML (2010). Beta1 integrin establishes endothelial cell polarity and arterial lumen formation via a Par3-dependent mechanism. *Dev Cell* 18, 39–51.